A CONTINUOUS, IN-CHAMBER TARGET TRACKING AND ENGAGEMENT APPROACH FOR LASER FUSION

Ron Petzoldt[1], Neil Alexander[1], Lane Carlson[2], Graham Flint[1], Dan Goodin[1], Jon Spalding[2], Mark Tillack[2]

[1]*General Atomics, San Diego, CA* Ronald.Petzoldt@gat.com
[2]*University of California San Diego, La Jolla, CA* mtillack@ucsd.edu

Target engagement is the process of measuring the target trajectory and directing the driver beams to hit the target at a position that is predicted based on these measurements. New target engagement concepts have been proposed in the last few years to continuously track the targets and to verify that the tracking system is aligned with the driver beams for each shot.

For transverse position, a laser beam continuously backlights the target and the position of the Poisson spot in the center of the target's shadow is measured. Axial target displacement is measured using a laser interferometer and counting interference fringes as the target moves away from the laser source. Final steering corrections use a "glint" reflected off the target ~1 ms prior to firing the laser beams and collected in a separate Position Sensitive Detector (PSD) for each driver beamlet. The position of the glint on the PSD is compared to the position of an alignment beam that is collinear with the driver beam. Steering corrections are then made based on the difference in position of the two spots reaching the PSD.

I. INTRODUCTION

Targets must be injected into an Inertial Fusion Energy (IFE) reaction chamber several times each second. Direct-drive targets must be hit by driver beams with an accuracy of ~20 μm. To achieve this accuracy, targets must be accurately tracked in all three dimensions and a means provided to ensure the driver beams can be directed to the target position. There must be a means of aligning the driver beam frame of reference with the tracking system. Frequent or continuous target position measurements allow the driver beam steering mirrors' positions to be continuously corrected as the target proceeds into the chamber. We are developing continuous target tracking methods for both transverse and axial target position and a "glint" target position feedback system for final alignment of the driver beams with the target.

II. TRANSVERSE POSITION MEASUREMENT

The ideal tracking system is one in which target position is defined in terms of displacement from, and location along, a line which joins a pair of fixed points that lie on diametrically opposite sides of the chamber.

The transverse tracking system layout is shown in Fig. 1. Here, to minimize the transverse motion caused by gravity, the targets are launched vertically downward along an axis which runs through the center of the chamber. Position sensing is accomplished by way of a laser beam which is coaxial to the capsule trajectory. Reference apertures on both sides of the chamber are used to align the tracking beam. As will be shown, the colinearity of these apertures with respect to a line which joins the center of the first reference aperture with the center of the centroid sensor can be established with great accuracy.

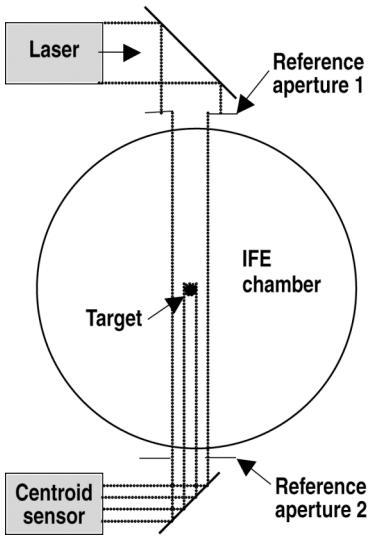

Fig. 1. Transverse tracking beam layout.

To detect small radial departures of the capsule with respect to the reference axis, advantage is taken of an optical phenomenon which variously is referred to as the

Poisson spot or the Spot of Arago. When a sharp-edged circular obscuration is centered within a collimated Gaussian beam, it creates an intense diffraction spot which is precisely centered upon the obscurations' shadow and which exists for all points within the near field [1]as shown in Fig. 2.

The size of the Poisson spot is dependent on the wavelength of the light used and the distance between the target and the detector location. At a distance, z, behind the obscuration the intensity of the field on or near the axis can be approximated well inside the geometric shadow by:[2]

$$I(r,z) = 0.5\tilde{u}(r,z)\overline{\tilde{u}(r,z)} \tag{1}$$

$$\tilde{u}(r,z) \approx -\frac{\tilde{q}_0}{\tilde{q}(z)} e^{-j\pi N - a^2/w_0^2} e^{-j\pi N(r/a)^2} J_0(2\pi N r/a)$$

where the over-bar represents the complex conjugate, r is the distance off axis, $\tilde{q}_0 = j\pi w_0^2/\lambda$, N is the Fresnel number ($N(z) = a^2/z\lambda$), λ is the wavelength, a is the radius of the obscuration and w_0 defines the width of the Gaussian beam. An example calculation for a target to sensor distance of 7 m is given in Fig. 3. The central spot diameter grows as the distance between the obscuration and the detector increases.

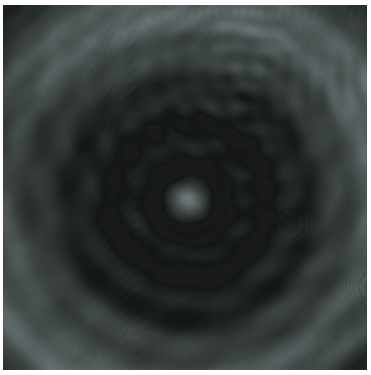

Fig. 2. Poisson spot (central bright spot) from 4 mm sphere illuminated with HeNe laser. The sphere is 4 m from the camera and the field of view is 5 mm × 5 mm.

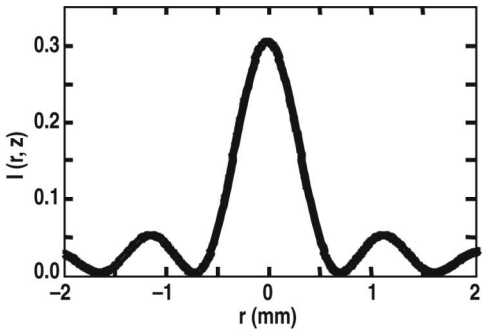

Fig. 3. Poisson spot intensity distribution for r = 2 mm, λ = 0.532 μm, w_0= 4 mm, and z = 7 m.

In the absence of a capsule, near-field diffraction patterns which are associated with the two reference apertures are superimposed upon the centroid detector. However, in contrast to a Poisson spot (which exhibits a strong central maximum at all distances within the near field), the centers of these patterns can exhibit either maxima or minima, depending upon the Fresnel number. Specifically, when the Fresnel number is an even integer, the pattern exhibits a sharply defined central null; when an odd integer, it exhibits a sharp maximum. Because the two apertures lie at substantially different distances from the centroid sensor, the Full Width Half Max (FWHM) values associated with their associated maxima/minima also differ. Consequently, by adjusting their Fresnel numbers, we can arrange for the more distant aperture to produce a relatively broad null, while the closer aperture produces a narrow maximum. Under these circumstances, the achievement of perfect alignment between the two apertures and the centroid sensor yields a minimum that takes the form of a rotationally symmetric annulus that is centered upon the centroid sensor. It is believed that this phenomenon can provide extremely precise alignment of the three reference points that form the basis of a colinear alignment scheme.

Our transverse target tracking laboratory tests as well as our entire integrated tabletop demonstration of the concepts in the paper are further described in Ref. 3.

III. LONGITUDINAL POSITION MEASUREMENT

To provide the axial position of a capsule, the Poisson spot tracking system can be supplemented by an optical fringe counting system. An optical fringe counting system offers the potential for extreme range accuracy, insofar as it defines the distance traveled by a target in terms of an integer multiplied by a laser wavelength; i.e. by a pair of quantities that can be established with extreme accuracy. However, since the process is based upon fringe counting, it is required that the detector must generate a few tens of photoelectrons from each fringe, this being a sufficient number that the probability of missing a fringe becomes negligible. Thus, we first must establish its viability by an examination of the photoelectron count rate at its detector.

The rate of photon production in the tracking beam is

$$N_{pT} = W\lambda/hc \tag{2}$$

where W is the laser power, λ is the laser wavelength, h is Planck's constant, c is the velocity of light. The fraction reaching the target for a uniform intensity beam (leaving beam splitter and other reflection losses for later) is

$$f_t = \frac{4r^2}{d^2} \tag{3}$$

where r is the target radius and d is the tracking beam diameter. The fraction of intercepted photons reaching the target that returns to the detector (neglecting reflection and transmission losses) is

$$f_d = \frac{\pi(D/2)^2}{4\pi z^2} = \frac{D^2}{16z^2} \quad (4)$$

where D is the diameter of the transmit/receive aperture and z is the distance to the target. Finally the number of photo-electrons produced assuming that an equal number returns from the reference leg is

$$N_e = 2N_{pT} f_t f_d \varepsilon T = \frac{\varepsilon T r^2 D^2 \lambda W}{2d^2 hcz^2} \quad (5)$$

where ε is the detector quantum efficiency, T is the collective optical transmission/reflection, and r is the radius of the target.

For an integrated acceleration and tracking system, the various parameters of equation (5) can be assigned values as follows:

Detector quantum efficiency	ε	0.5
Collective transmission/reflection	T	0.2
Target radius	r	2 mm
Tracking beam diameter	d	7 mm
Diameter of transmit/receive optics	D	10 mm
Planck's constant	h	6.6×10^{-34} J-s
Velocity of light	c	3×10^{8} m/s
Laser wavelength	λ	1.5 μm
Maximum target range	z	15 m

From which we find that the photoelectron count rate is approximately 1.37×10^{10} W/s.

A fringe counting interferometer yields one fringe for a distance change of λ/2. Hence, for a wavelength of 1.5 μm, such an interferometer has a range resolution of 0.75 μm. At 100 m/s, the corresponding fringe-to-fringe arrival time is 7.5 ns. The number of photoelectrons per fringe is 103 W. As previously noted, a few tens of photoelectrons per fringe are required for error-free counting. As a consequence, the laser power required for a simple fringe counting system becomes approximately 200–300 mW.

A greater signal to noise ratio can be achieved if the reference leg has higher intensity than the return signal from the target (as it normally will).

As the distance between the target and the interferometer changes, the curvature of the wave front also changes. However, the interferometer reference leg wave front curvature is normally constant. This causes the size of the central fringe of the interference pattern to change with target distance and makes counting the fringes much more difficult. One solution to this is to use a detector aperture that is smaller than the central fringe for all distances, but this reduces the usable signal. Additionally, if the target moves off axis, the position of the central fringe also moves. These two effects affect the robustness of the fringe counting method to changes in target position and have so far made implementation of this method of axial tracking difficult. Our experimental work on the fringe counting method is described in Ref. 4.

Since fringe-counting systems provide only differential position, rather than absolute position, the above described scheme requires an auxiliary sensor to provide a t_0 signal when the capsule passes a precisely defined point in its trajectory. In the layout presented in Fig. 4, this function is served by a laser and t_0 sensor that are located immediately adjacent to the outer wall of the chamber. Thus, while a line extending from a nearby aperture stop to the centroid sensor is used to define radial errors, the axial intercept of the t_0 crossing sensor is used to define axial errors.

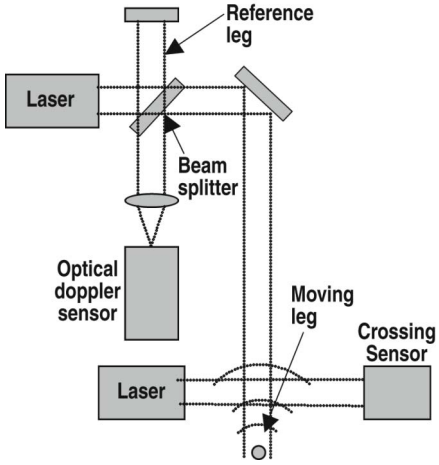

Fig. 4. Axial tracking beam layout utilizes Michelson interferometer with the target as the endpoint of the moving leg.

In Fig. 5, we show the Poisson spot distribution for a target to detector separation of 0.5 m. The small diameter of the Poisson spot, when used in conjunction with a narrow slit located in front of a detector, enables high-accuracy position measurement relative to an axial reference point. Two widely spaced crossing detectors can be used to measure target axial position and velocity. Position and velocity information can be used to predict target arrival time at the chamber center, but any unpredictable velocity changes due to chamber gas will adversely affect the prediction accuracy. Thus, although it represents a more easily implemented approach, it

nevertheless is considered to be a backup method to the fringe counting approach.

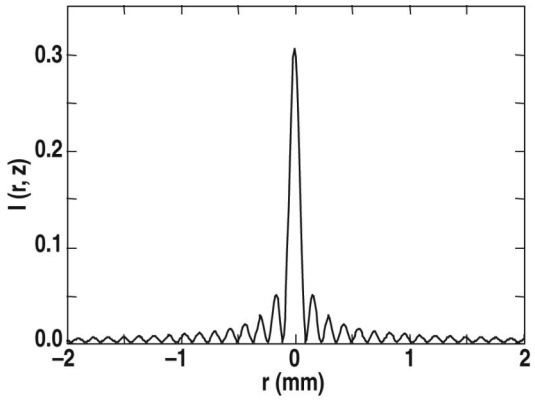

Fig. 5. Poisson spot intensity distribution for r = 2 mm, $\lambda = 0.532$ μm, $w_0 = 4$ mm, and z = 0.5 m.

III. TRACKING AND DRIVER BEAM ALIGNMENT

The ultimate objective of an injection and tracking system is to ensure that the point of aim for all laser beams coincides precisely in space and time with the center of a target capsule. The KRF laser with wavelength 248 nm is a leading candidate driver for an IFE power plant.[5] A KRF driver would simultaneously illuminate the target with about 60 driver beams, each of which is composed of about 50 beamlets.

A challenging task is to ensure that each of these driver beamlets and the target tracking system remain aligned to a common reference. This is especially true considering that the driver beams travel many 10's of meters and must hit the target with 20 μm accuracy. This must all be accomplished in the potentially high-vibration environment of an IFE power plant.

To achieve this alignment, we use the target itself as a common reference point for both systems. The overall conceptual layout is shown in Fig. 6. An alignment laser beam (with wavelength longer than 248 nm) propagates along the same beam paths as the driver beamlets. Each alignment beam reflects off of a segmented vacuum window into a cat's eye retro-reflector. The alignment beam is directed from the retro-reflector into a coincidence sensor which incorporates a position sensitive detector (PSD). Steering mirrors keep the alignment beam centered in the PSD.

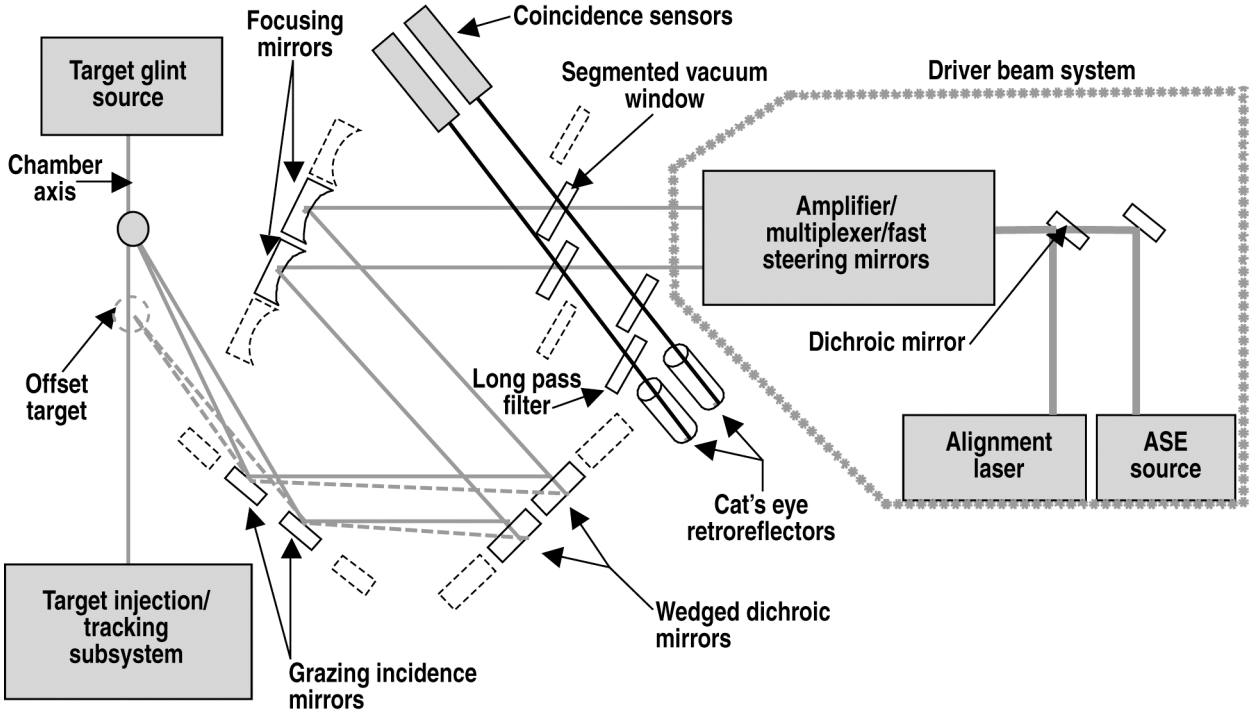

Fig. 6. Glint and beam steering system layout.

Approximately 1 ms before the target reaches the chamber center, a glint laser is pulsed to illuminate the target. The target reflects the glint light uniformly into 4 π steradians. Each coincidence sensor views the glint via the rear surface of a wedged dichroic mirror. Disparities between the beamlet alignment and the glint signals are used to reposition a fast steering mirror. Other than passing through the monolithic dichroic mirror, the glint beam follows the same optical path as the driver beam and alignment beam. The small ~ 1 mrad wedge angle is designed to precisely compensate for both the distance that the target will travel prior to driver beam arrival and for the offset between the position that the glint light reflects off of the target and the target center. The glint offset "*a*" (Fig. 7) is given by:

$$a = r \sin\Theta/2 \qquad (3)$$

where r is the target radius and Θ is the angle between the incident and reflected glint beam. For negligible error as Θ approaches π, the uncertainty in target radius must be <5 μm. If it is not possible to manufacture targets meeting this radius specification, it will be necessary to measure the radius of each target prior to or during injection and to compensate for the variance in offset with beam steering.

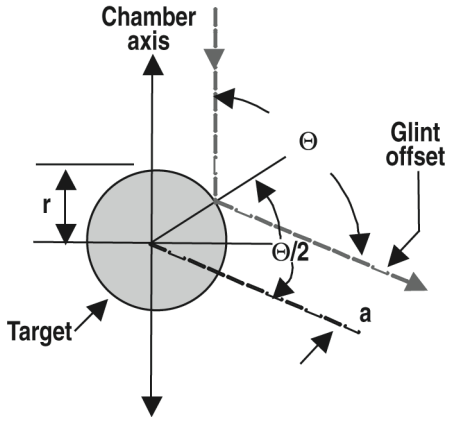

Fig. 7. The glint reflection is offset from the target center.

There are two beam steering scenarios under consideration. In the first scenario, the steering mirrors are repositioned continuously as transverse target position measurements become available from the Poisson spot detectors. This reduces the distance that the driver beams must be steered in the final ~1 ms after the glint. As higher speed beam steering methods become available and target injection accuracy improves, it may be possible to accomplish all the required beam steering after the glint signal arrives at the coincidence sensor.

IV. CONCLUSIONS

Continuous target tracking transverse to the injection axis can be measured with a Poisson spot detection system. Interference fringe counting together with a crossing sensor has the potential to continuously and accurately measure target axial position. However, implementation has proven to be difficult. Alternatively, it may be possible to rely on data from a pair of crossing sensors to predict target arrival time. As the target arrives at a position ~1 ms away from the chamber center, a glint laser beam will be pulsed. The reflection from the glint beam arrives via a wedged dichroic mirror to coincidence sensors (PSD) for each driver beamlet. The difference in position of the glint returns and alignment beams is used to reposition fast steering mirrors that direct the driver beamlets to hit the target. Thus the driver beam mirrors initally are steered by data derived from transverse/axial tracking systems and subsequently undergo fine adjustment relative to the actual target position ~1 ms prior to firing the driver beam.

ACKNOWLEDGMENTS

Work supported by NRL Contract N00173-06-C-6005.

REFERENCES

1. E. HECHT and A. ZAJAC, *Optics,* p. 374, Addison-Wesley, Menlo Park, CA (1974).

2. A.E. SIEGMAN, *Lasers,* pp. 734-736, University Science Books, Sausalito, CA (1986).

3. L.C. CARLSON, N.B. ALEXANDER, G. FLINT, D.T. GOODIN, T. LORENTZ, R.W. PETZOLDT, and M. TILLACK, "Target Tracking and Engagement Table-Top Demonstration," *17th ANS Topical Meeting on the Technology of Fusion Energy*, Albuquerque, NM, 2006, to be published in *Fusion Science and Technology.*

4. J. SPALDING, N.B. ALEXANDER, L.C. CARLSON, D.T. GOODIN, R.W. PETZOLDT, and M. TILLACK, "Longitudinal Target Tracking for Inertial Fusion," *17th ANS Topical Meeting on the Technology of Fusion Energy*, Albuquerque, NM, 2006, to be published in *Fusion Science and Technology.*

5. J.D. SETHIAN, *et al*., "Fusion Energy with Lasers, Direct Drive Targets, and Dry Wall Chambers," *Nuclear Fusion* **43** (2003) 1693-1709.